

Flattened velocity dispersion profiles in Globular Clusters: Newtonian tides or modified gravity?

X. Hernandez, M. A. Jiménez, C. Allen

Instituto de Astronomía, Universidad Nacional Autónoma de México, Apartado Postal 70–264, C.P. 04510 México D.F. México.

Released 21/06/2012

ABSTRACT

Over the past couple of years, a number of observational studies have confirmed the flattening of the radial velocity dispersion profiles for stars in various nearby globular clusters. As the projected radial coordinate is increased, a radius appears beyond which, the measured velocity dispersion ceases to drop and settles at a fixed value, σ_∞ . Under Newtonian gravity, this is explained by invoking tidal heating from the overall Milky Way potential on the outer, more loosely bound stars, of the globular clusters in question. From the point of view of modified gravity theories, such an outer flattening is expected on crossing the critical acceleration threshold a_0 , beyond which, a transition to MONDian dynamics is expected, where equilibrium velocities cease to be a function of distance. In this paper we attempt to sort out between the above competing explanations, by looking at their plausibility in terms of a strictly empirical approach. We determine Newtonian tidal radii using masses accurately calculated through stellar population modelling, and hence independent of any dynamical assumptions, distances, size and orbital determinations for a sample of 16 globular clusters. We show that their Newtonian tidal radii at perigalacticon are generally larger than the radii at which the flattening in the velocity dispersion profiles occurs, by large factors of 4, on average. While this point makes the Newtonian tidal explanation suspect, it is found that the radii at which the flattening is observed on average correlate with the radii where the a_0 threshold is crossed, and that σ_∞ values scale with the fourth root of the total masses, all features predicted under modified gravity theories.

Key words: gravitation — stellar dynamics — stars: kinematics — globular clusters: general

1 INTRODUCTION

The central values of the stellar velocity dispersion, projected on the plane of the sky, for many Galactic globular clusters (GC) have been well known for decades, and are known to accurately correspond to the expectations of self-consistent dynamical models under Newtonian gravity, e.g. King models (e.g. Binney & Tremaine 1987, Harris 1996). Recently, a number of studies (e.g. Scarpa et al. 2007a, 2007b, 2010 & 2011 and Lane et al. 2009, 2010a, 2010b & 2011, henceforth the Scarpa et al. and Lane et al. groups respectively) have performed measurements of the projected velocity dispersion along the line of sight for stars in a number of Galactic GCs, but as a function of radius, and reaching in many cases out to radial distances larger than the half-light radii of the clusters by factors of a few.

The surprising result of the above studies has been that radially, although velocity dispersion profiles first drop along Newtonian expectations, after a certain radius, settle to a

constant value, which varies from cluster to cluster. This behaviour is what is expected under MOND (Milgrom 1983), where equilibrium velocities tend to a constant value when below a critical acceleration, a_0 . In fact, such a result is fairly generic to modified theories of gravity designed to explain galactic rotation curves in the absence of any dark matter, e.g. Milgrom (1994), Bekenstein (2004), Zhao & Famaey (2010), Bernal et al. (2011), Mendoza et al. (2011), Capozziello & De Laurentis (2011). As already noted by Scarpa et al. (2011), it is suggestive of a modified gravity scenario that the point where the velocity dispersion profiles flatten, approximately corresponds to the point where average stellar accelerations drop below a_0 . Several recent studies have shown dynamical models for self-gravitating populations of stars under MOND or other modified gravity variants (e.g. Moffat & Toth 2008, Haghi et al. 2009, Sollima & Nipoti 2010, Haghi et al. 2011, Hernandez & Jiménez 2012) which accurately reproduce not only the observed velocity

dispersion profiles, but also the observed surface brightness profiles of observed GCs.

A recent study reaching the same conclusions, but at a significantly distinct scale, can be found in our work Hernandez, Jiménez & Allen (2012), where we show that the relative velocity of wide binaries in the solar neighbourhood is in conflict with predictions from full galactic dynamical simulations of the systems observed, and actually shows also velocities which cease to drop with distance, precisely on crossing the same a_0 threshold. Along the same lines, Lee & Komatsu (2010) show that the infall velocity of the two components of the Bullet cluster, as required to account for the hydrodynamical shock observed in the gas, is inconsistent with expectations of full cosmological simulations under standard Λ CDM assumptions. This has recently been confirmed at greater detail by Thompson & Nagamine (2012), and can in fact be seen as a failure not only of the Λ CDM model, but of standard gravity, as the required collisional velocity is actually larger than the escape velocity of the combined system. We note also the recent reviews by Kroupa et al. (2010), Famaey & McGaugh (2012) and Kroupa (2012) and references therein, detailing a number of observations in tension with standard Λ CDM assumptions.

From the point of view of assuming Newtonian gravity to be exactly valid at all low velocity regimes, it has also been shown that both velocity dispersion and surface brightness profiles for Galactic GCs can be self-consistently modelled. Under this hypothesis, it is dynamical heating due to the overall Milky Way potential that is responsible for the flattening of the velocity dispersion profiles e.g. Drukier et al. (2008), Küpper et al. (2010), Lane et al. (2010). The constant velocity dispersion observed at large radii merely shows the contribution of unbound stars in the process of evaporating into the Milky Way halo. In attempting to sort between these two contrasting scenarios, here we take a fully empirical approach. We critically examine the plausibility of both gravitational scenarios by looking through the data for other correlations which each suggest.

For the Newtonian case, we examine the best available inferences for the tidal radius of each cluster at closest galacto-centric passage, and compare it to the observed point where the velocity dispersion flattens. Here we find the former to generally exceed the latter by factors of 4 on average, making the Newtonian interpretation suspect. Also, we take all the clusters which the Lane et al. group have claimed show no indication of a modified gravity phenomenon, based on the fact that their velocity dispersion profiles can be modelled using Plummer profiles, and show that the fits with the generic asymptotically flat profiles we use are actually slightly better, in all cases.

From the point of view of MONDian modified gravity theories, we reexamine in greater detail the correlation between the crossing of the a_0 threshold and the point where the velocity dispersion flattens, already suggested by Scarpa et al. (2011). We shall use the term MONDian to refer to any modified theory of gravity which reproduces the basic phenomenology of MOND in the low velocity limit for accelerations below a_0 , of flat equilibrium velocities and a Tully-Fisher relation, regardless of the details of the fundamental theory which might underlie this phenomenology.

In consistency with the expectations of such theories, we find that mostly, systems almost fully within the $a < a_0$

threshold show almost fully flat velocity dispersion profiles, while those which only reach this threshold at their outskirts, present a significant Newtonian region, with a large fall in their velocity dispersion profiles. The above correlations are actually what would be expected generically under modified gravity schemes. We confirm our previous results with a much smaller sample of Hernandez & Jiménez (2012), showing that the asymptotic values of the velocity dispersion profiles are consistent with scaling with the fourth root of the total masses, a Tully-Fisher relation for GCs. Our results support the interpretation of the observed phenomenology as evidence for a change in regime for gravity on crossing the a_0 threshold.

In section (2) we present the detailed velocity dispersion fitting procedure, and show the best fit profiles, including a comparison with the Plummer models used by the Lane et al. group, which are slightly worse than the asymptotically flat profiles we use. A description of the tidal radii derivations and the calculation of the confidence intervals for all the globular cluster parameters used is also given. Section (3) shows a comparison of the tidal radii against the radii at which the velocity dispersion becomes flat, as a test of the plausibility of Galactic tides under a Newtonian scenario as responsible for the observed outer flattening of the velocity dispersion profiles. In section (4) we present a number of scalings between the structural parameters of the observed globular clusters, showing these systems to be consistent with MONDian gravity expectations, in terms of a change towards a modified regime on crossing the a_0 threshold. Our conclusions are summarised in section (5).

2 EMPIRICAL VELOCITY DISPERSION MODELLING

We begin by modelling the observed projected radial velocity dispersion profiles, $\sigma_{obs}(R)$, in the globular clusters in our sample, listed in table 1. As seen from the Scarpa et al. and Lane et al. data, the observed velocity dispersion profiles show a central core region where the velocity dispersion drops only slightly, followed by a “Keplerian” zone where the drop is more pronounced. These first two regions are in accordance with standard Newtonian King profiles, but they are then followed by a third outermost region where the velocity dispersion profiles cease to fall along Keplerian expectations, and settle to fixed values out to the last measured point. As some of us showed in Hernandez & Jiménez (2012), an accurate empirical modelling for these velocity dispersion profiles can be achieved through the function:

$$\sigma(R) = \sigma_1 e^{-(R/R_\sigma)^2} + \sigma_\infty \quad (1)$$

In the above equation σ_∞ is the asymptotic value of $\sigma(R)$ at large radii, R_σ a scale radius fixing how fast the asymptotic value is approached, and σ_1 a normalisation constant giving $\sigma(R=0) = \sigma_1 + \sigma_\infty$.

We now take the observed data points $\sigma_{obs}(R_i)$ along with the errors associated to each data point, to determine objectively through a maximum likelihood method the best fit values for each of the three parameters in equation (1), for each of the 16 observed globular clusters. Assuming the errors to have a Gaussian distribution, the likelihood function will be:

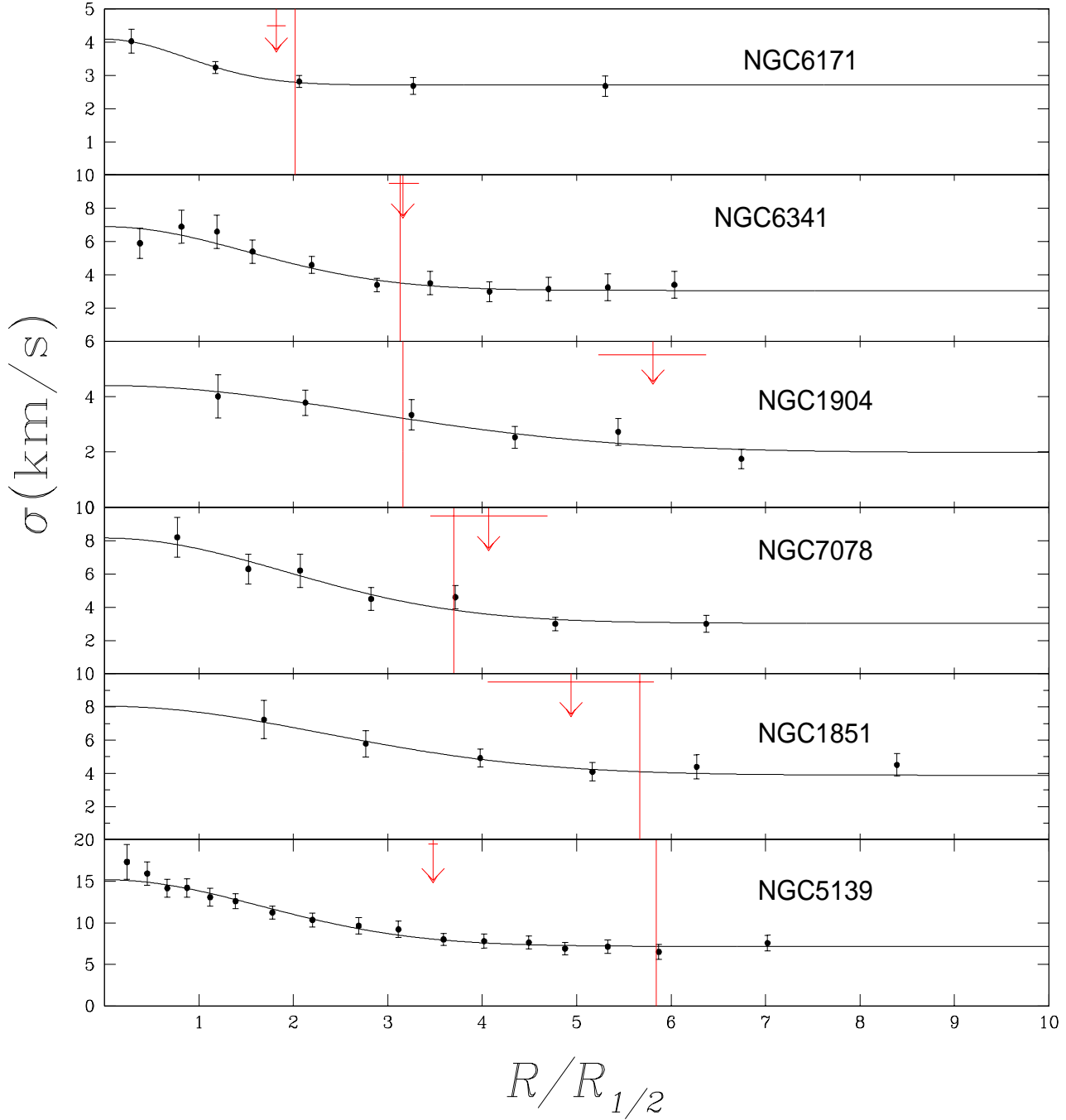


Figure 1. The figure shows the observed projected velocity dispersion profiles for six GCs in the Scarpa et al. sample, points with error bars, as a function of the radial coordinate, normalised to the half-light radius of each. The solid curves give the maximum likelihood fits to the asymptotically flat $\sigma(R)$ model of eq.(1), seen to be accurate descriptions of the data. The vertical lines indicate the $a = a_0$ threshold, and the arrows point where the profiles flatten, *a priori* independent features, in most cases seen to occur at approximately the same region; see text for details.

$$\mathcal{L}(\sigma_\infty, \sigma_1, R_\sigma; \sigma_{obs}(R_i)) = \prod_{i=1}^n \frac{\exp[-(\sigma_{obs}(R_i) - \sigma(R_i))^2 / 2\Delta_i^2]}{\Delta_i} \quad (2)$$

where Δ_i is the error on the i -th data point, and $\sigma(R)$ is a particular model resulting from a given choice of the three

model parameters. Thus, for any choice of the three model parameters, the likelihood function can be calculated for a given data set $\sigma_{obs}(R_i)$ with its errors. For each observed globular cluster, we calculate the likelihood function over a 100^3 grid in parameter space, and then select the point

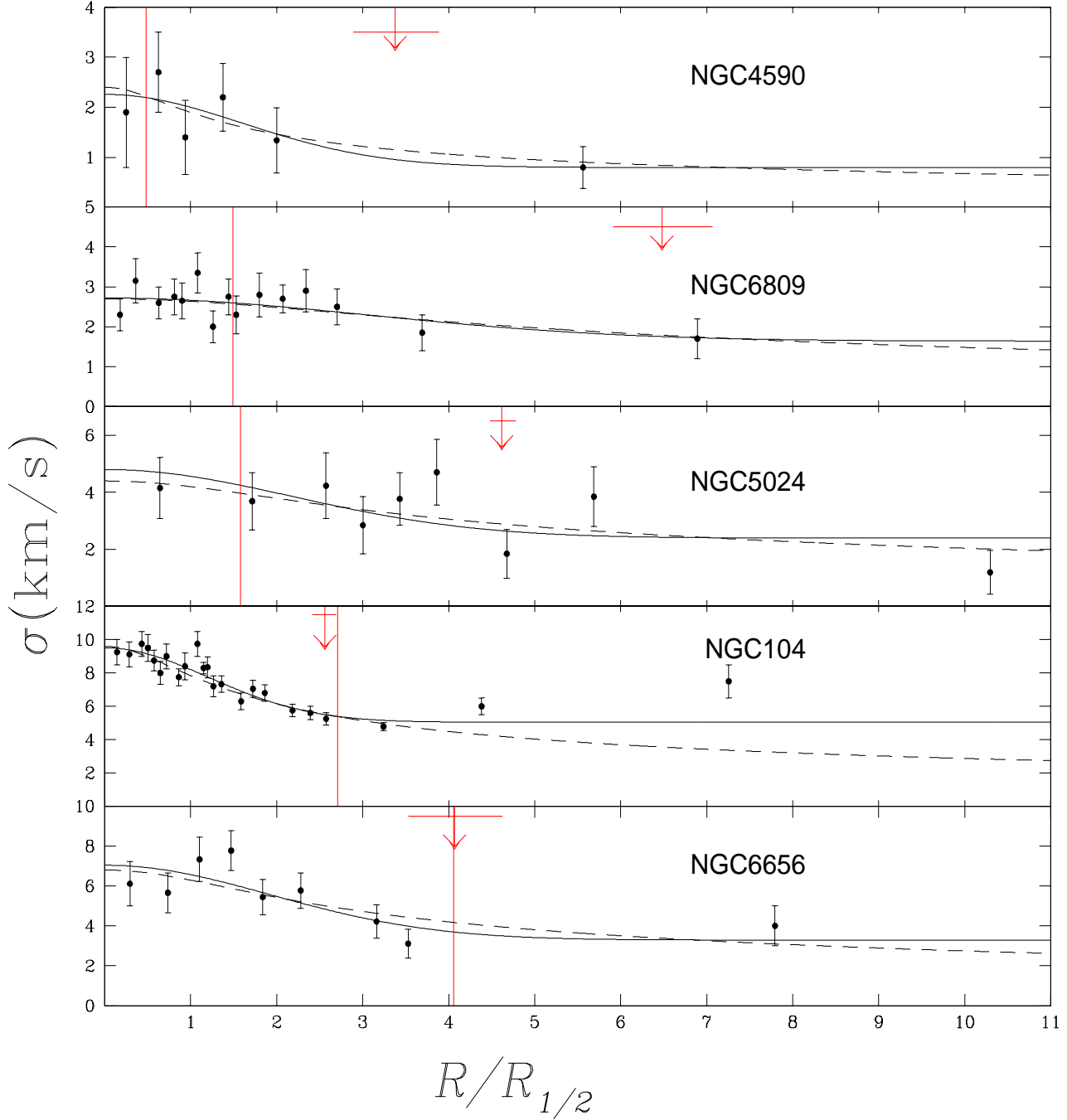


Figure 2. The figure shows the observed projected velocity dispersion profiles for five GCs in the Lane et al. sample, points with error bars, as a function of the radial coordinate, normalised to the half-light radius of each. The solid curves give the maximum likelihood fits to the asymptotically flat $\sigma(R)$ model of eq.(1), seen to be accurate descriptions of the data. The dashed lines give the best fit Plummer models from the Lane et al. papers, also fair representations of the data. The vertical lines indicate the $a = a_0$ threshold, and the arrows the point where the profiles flatten, *a priori* independent features, in most cases seen to occur at approximately the same region; see text for details.

where this function is maximised, to identify the optimal set of parameters for each observed velocity dispersion profile, $(X_{1,0}, X_{2,0}, X_{3,0})$. As it is customary, we work with the logarithm of the likelihood function. The confidence intervals for each of the three parameters are then obtained by looking

through the full likelihood matrix to identify the largest and smallest values for a particular parameter which satisfy the condition $\ln\mathcal{L}(X_{lim}, X_2, X_3) - \ln\mathcal{L}(X_{1,0}, X_{2,0}, X_{3,0}) = 0.5$, i.e., the full projection of the error ellipsoid is considered, without imposing any marginalisation. This last point al-

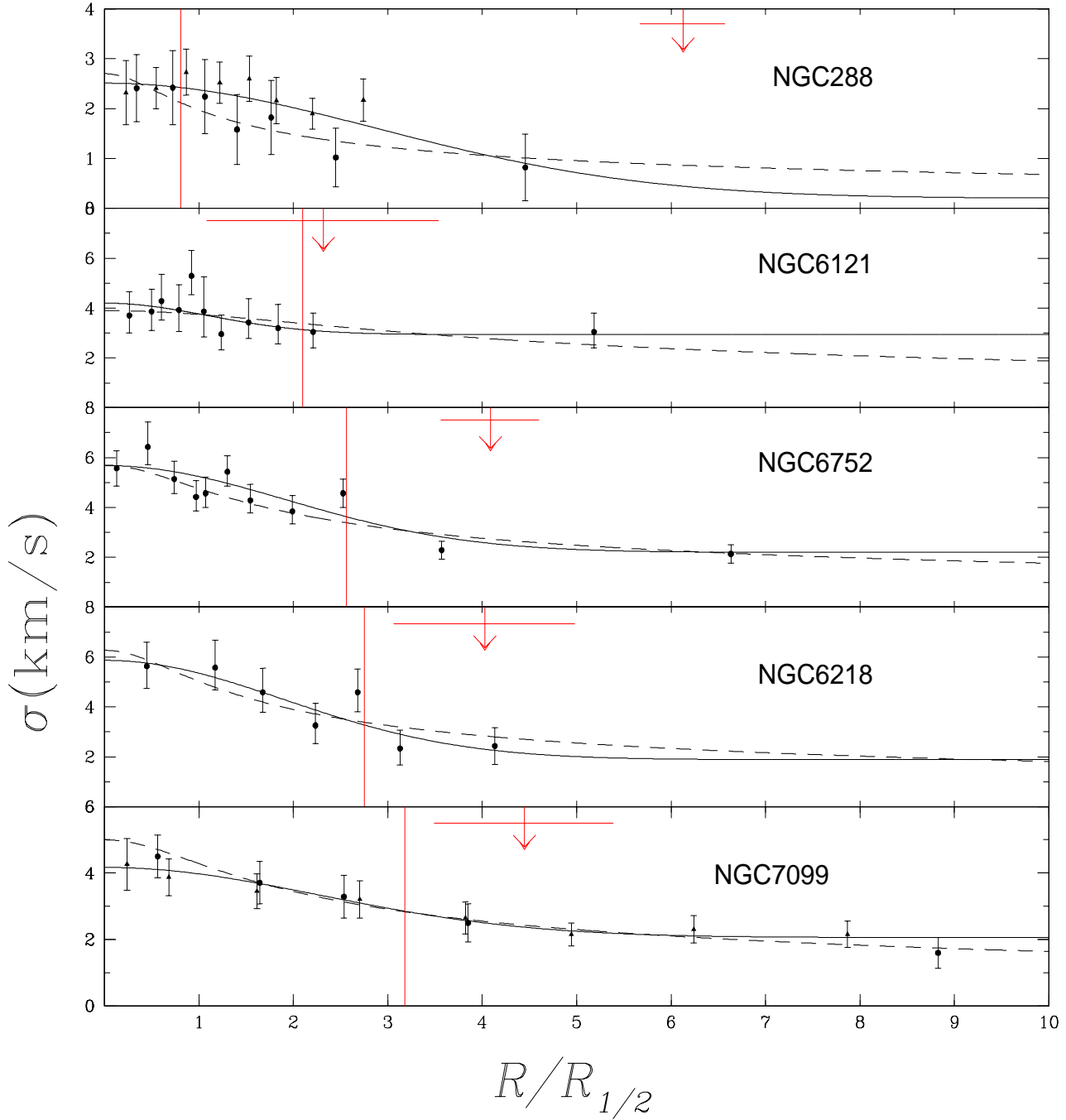


Figure 3. The figure shows the observed projected velocity dispersion profiles for the remaining five GCs in the Lane et al. sample, points with error bars, as a function of the radial coordinate, normalised to the half-light radius of each. The solid curves give the maximum likelihood fits to the asymptotically flat $\sigma(R)$ model of eq.(1), seen to be accurate descriptions of the data. The dashed lines give the best fit Plummer models from the Lane et al. papers, also fair representations of the data. NGC 288 and NGC 7099 are common to both samples, dots and triangles show the Lane et al. and Scarpa et al. data, respectively. The vertical lines indicate the $a = a_0$ threshold, and the arrows the point where the profiles flatten, *a priori* independent features, in most cases seen to occur at approximately the same region; see text for details.

lows to properly account for any correlations between the three fitted parameters when calculating any quantity derived from combinations of them, as will be constructed in what follows.

Taking $\sigma_{obs}(R_i)$ data from Drukier et al. (1998), Scarpa et al. (2004), (2007a), (2007b), (2010) and (2011), Lane et al. (2009), (2010a), (2010b) and (2011) and half-light radii, $R_{1/2}$, from integrating the surface density brightness profiles of Trager et al. (1995), we perform a maximum likelihood fit as described above for all the sixteen globular clusters studied.

Figure (1) shows the observed projected velocity dispersion profiles for the 6 globular clusters from the Scarpa et al. group, which are not also part of the Lane et al. total sample, points with error bars. The radial coordinate has been normalised to the $R_{1/2}$ radius of each of the clusters. The continuous curves show the maximum likelihood fits for each cluster, which are clearly good representations of the data. We can now give $R_f = 1.5R_\sigma$ as an adequate empirical estimate of the radius beyond which the dispersion velocity profile becomes essentially flat. In terms of equation (1), which can be seen to be highly consistent with the observed velocity dispersion profiles, R_f is the radius such that $\sigma(R_f) = 0.1\sigma_1 + \sigma_\infty$, a good representation of the transition to the flat behaviour, as can be checked from figure (1), where the arrows give R_f , with the horizontal lines on the arrows showing the 1σ confidence intervals on these fitted parameters. An empirical definition of the radius where the typical acceleration felt by stars drops below a_0 can now be given as R_a , where:

$$\frac{3\sigma(R_a)^2}{R_a} = a_0. \quad (3)$$

Using the above definition, we can now identify R_a for each of the globular clusters studied. The vertical lines in Figure(1) show R_a for each cluster, also normalised to the half-light radius of each. In the figure, clusters have been ordered by their $R_a/R_{1/2}$ values, with the smallest appearing at the top, and $R_a/R_{1/2}$ growing towards the bottom of the figure.

The Lane et al. sample comprises 10 clusters, two of which are also part of the Scarpa et al. sample. Figure 2 is analogous to Figure 1, and shows velocity dispersion profiles for 5 clusters from the Lane et al. sample not having any overlap with the Scarpa et al. group. Here we have added also the best fit Plummer models to the data, with parameters taken from the Lane et al. papers, and shown by the dashed curves. It is obvious that both functional forms provide good representations to the data, which qualitatively, display an asymptotically flat region at large radii. At large radii, the line of sight velocity dispersion profiles for the Plummer models fall to zero, but only very slowly, as $R^{-1/2}$. This allows good fits to data which qualitatively tend to constant values. The good fits allowed by the Plummer models are clearly not sufficient to dismiss a modified gravity interpretation, as the asymptotically flat projected dispersion velocity fits of the type used for full dynamical modelling under modified gravity (Hernandez & Jimenez 2012) are equally consistent with the data.

Figure (3) completes the fits to the Lane et al. sample, where NGC 6121, NGC 6218 and NGC 6752 are analogous to the ones shown in Figure 2. Again, the dashed and solid

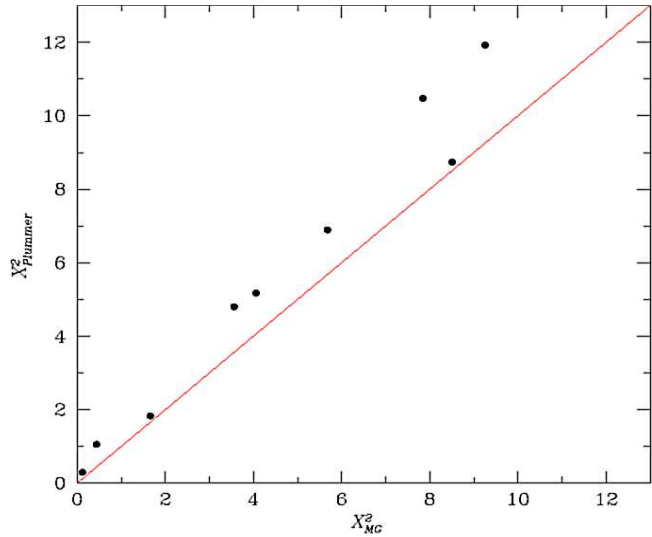


Figure 4. The figure shows a comparison of the χ^2 values for the best fit asymptotically flat $\sigma(R)$ model of eq.(1), and the optimum Plummer model fits from the Lane et al. papers to the same data samples. Although both fits are comparable as representations of the observed projected velocity dispersion profiles, the asymptotically flat model suggested by modified gravity schemes provides, in all cases, a slightly better description of the data.

curves are essentially equivalent. The remaining two clusters in this figure give the two examples which have been studied by both groups of observers, NGC 7099 and NGC288, where the triangles and dots with error bars give the Scarpa et al. and Lane et al. data, respectively. In these last two cases, the dashed lines give the best fit Plummer models from the Lane et al. papers, and the solid lines, the best fit models from eq. (1), considering joint data samples from both groups. An eq.(1) fit limited to the Lane et al. data for these last two clusters was also performed, for the comparison shown in the following figure. For the last two clusters, we see that the two independent data samples are consistent with a fixed underlying distribution, and also, that the fits to the added samples from eq.(1), represent the data as well as the Plummer models.

It is interesting at this point to notice a first correlation, the smaller the value of $R_a/R_{1/2}$, the larger the fraction of the cluster which lies in the $a < a_0$ regime, and interestingly, the flatter the velocity dispersion profile appears. At the top of the figures we see clusters where stars experience accelerations below a_0 almost at all radii, and it so happens, that it is only in these systems that the velocity dispersion profile appears almost flat throughout. Towards the bottom, we see systems where only at the outskirts accelerations fall under a_0 . Over most of their extents, these clusters lie in the Newtonian $a > a_0$ regime, and indeed, it is exclusively these, that show a clear Keplerian decline in the projected velocity dispersion profiles over most of their extents. Also, notice that on average, R_f and R_a approximately coincide, as already previously noticed by Scarpa et al. (2007a), the flattening in the velocity dispersion profiles seems to appear on crossing the a_0 threshold.

We end this section with Figure (4) which compares the χ^2 values for the Plummer fits to the Lane et al. data, to the χ^2 values for the eq.(1) fits to the same data. As it was already obvious from figures (2)-(3), both functional forms provide fits of very similar quality, although a rigorous statistical assessment actually shows the fits to profiles

which are asymptotically flat at large radii to better represent the data than the Plummer models, which slowly tend to zero. NGC 104, which results in the poorest fits under both functional forms tested, falls off the range shown in Figure (4). For the asymptotically flat profile suggested by MONDian gravity schemes, this cluster yields a χ^2 value of 28.55, while for the Newtonian Plummer profile of Lane et al., a χ^2 of 51.14 results. This cluster is in fact the one for which the difference in χ^2 values is greatest, in the sense of further supporting the conclusions presented, but was omitted from the figure to allow greater detail in the region where the majority of the clusters lie.

3 TESTING THE NEWTONIAN EXPLANATION

In order to test the validity of the explanation for the outer flattening of the observed velocity dispersion profiles under Newtonian gravity, that these indicate dynamical heating due to the tides of the Milky Way system (bulge plus disk plus dark halo), we need accurate estimates of the Newtonian tidal radii for the clusters studied. One of us in Allen et al. (2006) and Allen et al. (2008) performed detailed orbital studies for 54 globular clusters for which absolute proper motions and line of sight velocities exist. In that study, both a full 3D axisymmetric Newtonian mass model for the Milky Way and a model incorporating a galactic bar were used to compute precise orbits for a large sample of globular clusters, which fortunately includes the 16 of our current study. The Galactic mass models used in those papers are fully consistent with all kinematic and structural restrictions available. Having a full mass model, together with orbits for each globular cluster, allows the calculation of the Newtonian tidal radius, not under any “effective mass” approximation, but directly through the calculation of the derivative of the total Galactic gravitational force, including also the evaluation of gradients in the acceleration across the extent of the clusters, at each point along the orbit of each studied cluster.

The Newtonian tidal radii we take for our clusters, R_T , are actually the values which result in the largest dynamical heating effect upon the clusters studied, those at perigalacticon. As the distance of closest approach to the centre of the Galaxy might vary from passage to passage, as indeed it often does, detailed orbital integration is used to take R_T as an average for perigalactic passages over the last 1 Gyr.

We update the tidal radii published in Allen et al. (2006) and Allen et al. (2008), by considering revised total masses from the integration of the observed V band surface brightness profiles for our clusters (Trager et al. 1995), and using the V band stellar M/L values given in McLaughlin & van der Marel (2005) and accompanying electronic tables. For each individual GC, detailed single stellar population models tuned to the inferred ages and metallicities of each of the clusters we model were constructed in that study, using various standard population synthesis codes, and for a variety of assumed IMFs. In this way present stellar M/L values in the V band were derived, which we use here. As we do not in any way use the dynamical mass estimates of McLaughlin & van der Marel (2005), the total masses we use are independent of any dynamical modelling or assumption regarding the law of gravity, as they are derived

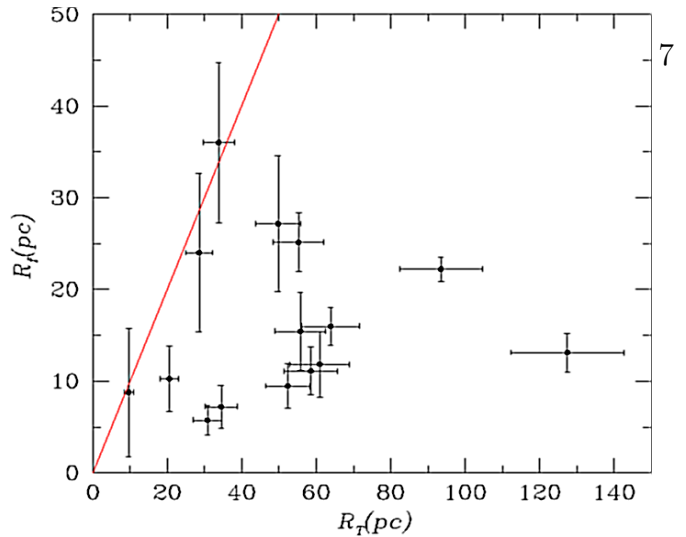


Figure 5. The figure shows the relation between the point where the velocity dispersion flattens, R_f , and the Newtonian tidal radius, R_T , for each cluster. Even considering the large errors involved on both quantities, on average points fall far to the right of the identity line shown, making the Newtonian explanation for the flattened velocity dispersion profiles, rather suspect.

through completely independent surface brightness profile measurements and stellar population modelling. The confidence intervals in our tidal radii include the full range of stellar M/L values given by McLaughlin & van der Marel (2005), through considering a range of ages, metallicities and initial mass functions consistent with the observed HR diagrams for each cluster. These uncertainties dominate the error budget on R_T , as those introduced by the observational uncertainties in the orbital determinations are much smaller. This last can be seen from the range in R_T values given in Allen et al. (2006) which are extreme in being derived from taking all four orbital parameters at their 1σ extremes, something with a probability of $(0.318)^4=1\%$, and are hence about 2.58σ ranges. Although sub-dominant, the corresponding 1σ errors on R_T have also been added. In what follows, we shall make use of total stellar masses derived as explained above, including as confidence intervals the full uncertainties in these results associated with the various IMFs assumed by the McLaughlin & van der Marel (2005), and not the much narrower confidence intervals resulting from taking a fixed IMF.

In Figure (5) we show values of R_f for our clusters, plotted against their corresponding R_T values, both in units of pc. The error bars in R_f come from the full likelihood analysis described in the fitting process of equation (1) to $\sigma_{obs}(R)$, which guarantees that confidence intervals in both of the quantities plotted are robust 1σ ranges. The solid line shows a $R_f = R_T$ relation. It is obvious from the figure that the onset of the flat velocity dispersion regime occurs at radii substantially smaller than the tidal radii, for all of the globular clusters in our sample. Even under the most extreme accounting of the resulting errors, only three of the clusters studied are consistent with $R_T \approx R_f$ at 1σ . Actually, the average values are closer to $R_T = 4R_f$, with values higher than 8 appearing. One of the clusters, NGC 5024 does not appear, as it has values of $R_T = 184.12$, $R_f = 36$, which puts it out of the plotted range, but consistent with the description given above. Given the R^3 scaling of Newtonian tidal phenomena, even a small factor of less than 2

inwards of the tidal radii, tides can be safely ignored, e.g. in Roche lobe overflow dynamics, the stellar interior is largely unaffected by the tidal fields, until almost reaching the tidal radius. It therefore appears highly unlikely under a Newtonian scheme, that Galactic tides could be responsible for any appreciable dynamical heating of the velocity dispersion of the studied clusters.

We note that Lane et al. (2010) and Lane et al. (2012) find that Newtonian tidal heating can explain the observed velocity dispersion profile of their GC sample. However, it is important to note that in Lane et al. (2010) and Lane et al. (2012), total masses were calculated directly from the observed velocity dispersion observations, under the assumption that Newtonian dynamics hold. If that assumption is to be tested, the importance of deriving total masses through an independent method, not based on stellar dynamics, is evident. Our results do not imply that the Newtonian explanation might not apply to other GCs, e.g. the theoretically constructed ones of Küpper et al. (2010) and Küpper et al. (2012), which show the Newtonian explanation to hold *in principle*, although no real GCs were included in those studies. A potential caveat of all the above studies is the use of strictly axisymmetric potentials for the Milky Way, given that in Allen et al. (2006) and Allen et al. (2008) it is shown that the orbital dynamics of Galactic globular clusters with orbits probing the regions where the Galactic bar is present, as many in our sample do, can be strongly affected by its presence.

Notice also, that most of the clusters in our sample are problematic for a Newtonian gravity scheme, even without the recent observations of an outer flat velocity dispersion profile. As remarked already in Allen et al. (2006), the clusters in our sample have Newtonian tidal radii larger than the observed truncation radii of their light distribution, the sole exceptions being Omega Cen (NGC 5139) and M92 (NGC 6341), two rather anomalous clusters. Whereas a full dynamical modelling under an extended gravity force law of these clusters, Hernandez & Jiménez (2012), naturally yielded an outer truncation for the light profile, under a Newtonian hypothesis, the observed truncation in the light profile of the clusters in our sample cannot be explained as arising from interaction with the tidal field of the Milky Way.

Furthermore, notice that we have taken R_T at perigalacticon, where tides are at their most severe over the clusters orbit, any other orbital occupation averaging would result in substantially larger R_T values. Notice also that as shown by Allen et al. (2006) and Allen et al. (2008), the inclusion of a realistic massive Galactic bar potential, in the case of the clusters in our sample, results generally in negligible changes in the resulting R_T values, or in some cases, a slight increase in these values. Hence, even taking the fullest non-axisymmetric Galactic mass model under Newtonian gravity, with precise orbits derived from 3D velocity measurements for the clusters studied, together with total mass determinations tuned to the individual stellar populations of them, yields tidal radii as shown in figure (2).

Regarding a comparison to the expectations under Newtonian gravity, an interesting dynamical effect appears when a stellar halo object is near its apocentre. As shown in e.g. Niederste-Ostholt et al. (2012), near apocentre tidal tails are compressed into what might look like a high dispersion velocity halo. We have checked the position of the clusters

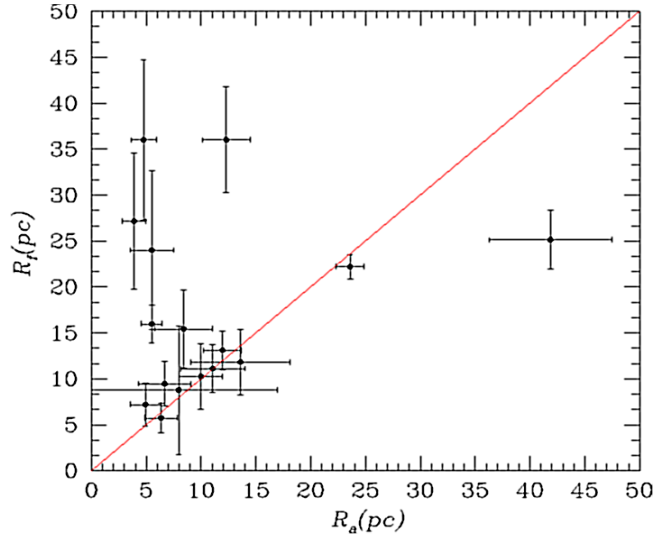


Figure 6. The figure gives the relation between the radius where the velocity dispersion flattens, R_f , and the point where average stellar accelerations fall below the a_0 threshold, R_a .

studied along their orbits, and found that only in the case of NGC 6121 is the cluster near apocentre, checked explicitly from the orbits for the clusters in question from Allen et al. (2006) and Allen et al. (2008). Notice that this case also follows the MONDian expectations of figure (7), see below. It is also important to note that the piling up of tidally stripped stars near apocentre has not been proven to hold for more chaotic orbits, and probably does so to a much smaller degree than what shown in Niederste-Ostholt et al. (2012) for a pure axisymmetric potential. This is relevant, as the orbits of clusters lying within the region of influence of the galactic bar, as many of the ones in our sample do, become substantially chaotic, with no well defined periodic apocentre distance, as shown in the Allen et al. papers mentioned.

4 TESTING A MODIFIED GRAVITY EXPLANATION

We begin this section by testing the correlation between R_a and R_f . As already noticed by Scarpa et al. (2011), the flattening in the observed velocity dispersion profiles seems to appear at the point where the a_0 threshold is crossed. Here we use the much more careful and objective modeling of the observed velocity dispersion curves of the previous section to test this point, shown in Figure (6).

We see 9 GCs in the sample falling within 1σ of the identity line shown, a further three lying within 2σ of this same line, and the remaining four appearing as outliers. Thus, the correlation appears stronger than in Figures (1)-(3), where errors on $R_a/R_{1/2}$ appear and only a qualitative comparison is implied, not including the confidence intervals in R_a . A quantitative test of the correlation being explored is possible, since the careful modelling of the velocity dispersion profiles we performed naturally yields objective confidence intervals for the parameters of the fit. Of the outliers, NGC288 presents an almost entirely flat velocity dispersion profile, and is hence a case where the parameter

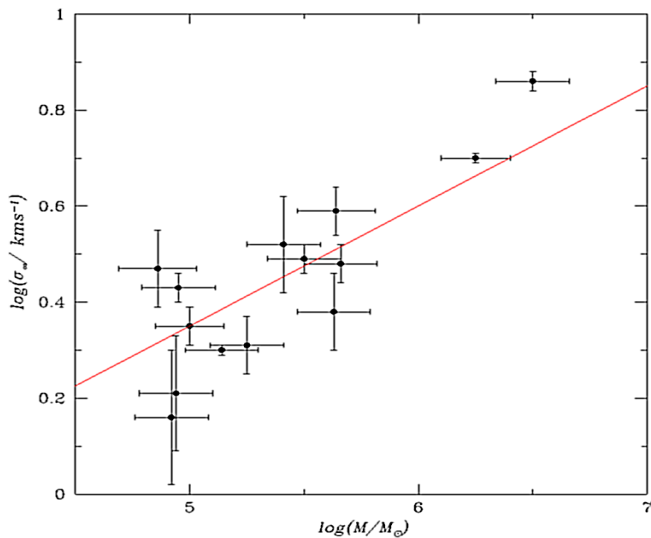


Figure 7. Here we give the relation between the observed asymptotic dispersion velocity measurements, and the total mass of each cluster. The line gives the best fit $\sigma \propto M^{1/4}$ scaling for the data, and is consistent with the galactic scale Tully-Fisher relation.

R_σ is only poorly constrained. In this figure we thus quantify the correlation between the point where the velocity profile flattens, and the crossing of the a_0 threshold, as expected under MONDian schemes, which is seen to hold on average. One could think of adding a point at (0,0) in Figure (6), corresponding to the local dSph galaxies, systems with fully isothermal observed velocity dispersion profiles, lying fully within the $a < a_0$ condition, e.g. Angus (2008), Hernandez et al. (2010). A possible caveat is the use of only a coarse definition for R_a , which relies only on projected quantities which are integrals along the line of sight. More detailed dynamical structure modelling of the type found in Hernandez & Jiménez (2012), requiring fixing on a particular modified gravity model, something which we expressly avoid in the present study, might reveal slight differences from the current Figure (6), perhaps with no outliers.

As already noticed in Figures (1)-(3), a correlation is evident in that the further out, in units of the cluster half-light radius, that the a_0 threshold is reached, the larger the relative drop in the observed velocity dispersion profile. This is expected under MONDian gravity schemes, since when the Newtonian $a > a_0$ region is larger within a particular cluster, the larger the “Keplerian” fall before the $a < a_0$ modified regime is reached.

We end this section with Figure (7), which shows the relation between the measured asymptotic velocity dispersion, σ_∞ , and the total mass of the clusters in question. The mass was calculated as described in section (3), and therefore represents the best current estimate of the stellar mass for each of the clusters in the sample, including its corresponding confidence intervals. As with all the other correlations and data presented in figures (1)-(6), there is no dynamical modelling or modified gravity assumptions going into the data presented in Figure (7), merely observable quantities. We see, as already pointed out in Hernandez & Jiménez (2012), that the GCs observed comply with a scaling of $\sigma \propto M^{1/4}$, the Tully-Fisher law of galactic systems “embedded within massive dark haloes”.

From this last figure two clusters have been excluded, NGC 288 and NGC 4590 which have very poorly determined σ_∞ values, with uncertainties so large that these clusters provide little information in terms of Figure (7). Regarding NGC 288, both the Scarpa et al. and the Lane et al. data are noisier than for the others. Also, taking only one set of data yields significantly distinct answers, although still barely within their respective errors, a low asymptotic velocity for the Lane et al. sample, a high value from the Scarpa et al. data. This does not happen with the other common GC, NGC 7099, where both data samples are in complete agreement. Although Sollima et al. (2012) recently reported a velocity dispersion profile for NGC 288, this is equally noisy, and does not help to clear the case, their data are actually consistent, to their respective errors, with both the Lane et al. or the Scarpa et al. data. Given the current level of observational uncertainties we prefer to exclude NGC 288 from any consideration regarding its asymptotic velocity value, until a clearer picture emerges from the observational point of view.

The straight line shows the best fit $\sigma \propto M^{1/4}$ scaling, and actually falls only a factor of 1.3 below the modified gravity prediction for systems lying fully within the low acceleration regime (e.g. Hernandez & Jiménez 2012), for the same value of $a_0 = 1.2 \times 10^{-10} m/s$ used here, as calibrated through the rotation curves of galactic systems. This small offset is not surprising, since the GCs treated here are not fully within the $a < a_0$ condition, most have an inner Newtonian region encompassing a substantial fraction of their masses. Notice also that from an statistical point of view, consistency of a set of data points with a model does not require for all data points to lie within 1σ of the proposed model. Probabilistically, one actually expects about 1/3 of the points to lie between 1σ and 2σ of the model, with 1/100 expected between 2σ and 3σ , even for data actually extracted from a given model. Given the size of our sample, finding 5 GCs without 1σ , but within 2σ of the proposed model is then well within expected random noise, inasmuch as we have taken care to ensure that the error bars given are real 1σ confidence intervals. Further, as many of the GCs in our sample have not reached acceleration values significantly below a_0 at their last measured point, while other have, a certain intrinsic scatter would be expected in Figure (7) from a MONDian gravity perspective.

From a Newtonian point of view, if Galactic tides were responsible for the observed outer flattening of the velocity dispersion profiles studied, given the narrow range of half light radii these present, and given the inverse scaling of Newtonian tides with the density of the satellite, a slight downward trend for decreasing asymptotic velocity dispersion with increasing mass would be expected in Figure (7). This would of course be blurred significantly by the range of perigalacticon distances inferred for the GCs in our sample. It is clear from the figure that a blurred decreasing trend is not what the data show; rather, consistency with the $\sigma \propto M^{1/4}$ of MONDian gravity, including the normalisation, is evident. A preliminary version of this last figure appeared already in Hernandez & Jiménez (2012); we reproduce here an updated version using now the extended sample of clusters treated, and σ_∞ values and their confidence intervals as derived through the careful velocity dispersion fitting procedure introduced.

Table 1. Parameters for the globular clusters treated.

GC	$\sigma_1(km/s)$	$\sigma_\infty(km/s)$	$R_\sigma(pc)$	$R_a(pc)$	$R_{1/2}(pc)$	$R_T(pc)$	$\log_{10}(M/M_\odot)$	b	$\Delta V_r(km/s)$
NGC 104 ²	4.5 ± 0.4	5.0 ± 0.1	14.8 ± 0.9	23.6 ± 1.3	8.7 ± 1	93.5 ± 11.1	6.3 ± 0.2	-45.20	-18.7
NGC 288 ^{1,2}	2.3 ± 1.4	0.2 ± 0.8	24.0 ± 5.8	4.8 ± 1.2	5.9 ± 1	33.8 ± 4.2	4.8 ± 0.2	-89.38	-46.6
NGC 1851 ¹	4.2 ± 3.0	3.9 ± 0.4	7.9 ± 2.4	13.6 ± 4.5	2.4 ± 1	60.9 ± 10.7	5.6 ± 0.2	-35.03	320.5
NGC 1904 ¹	2.4 ± 0.3	2.0 ± 0.1	10.3 ± 2.9	8.4 ± 2.6	2.7 ± 1	55.8 ± 9.4	4.9 ± 0.2	-29.35	206.0
NGC 4590 ²	1.5 ± 0.6	0.8 ± 0.4	18.1 ± 5.0	3.9 ± 1.1	8.0 ± 1	49.8 ± 6.0	5.7 ± 0.2	35.8	-94.3
NGC 5024 ²	2.4 ± 1.5	2.4 ± 0.5	24.0 ± 3.8	12.3 ± 2.2	7.8 ± 1	184.1 ± 22.2	5.6 ± 0.2	79.3	-62.9
NGC 5139 ¹	8.0 ± 1.0	7.2 ± 0.4	16.8 ± 2.1	41.9 ± 5.6	7.2 ± 1	55.3 ± 8.9	6.4 ± 0.2	14.97	232.3
NGC 6121 ²	1.3 ± 1.0	2.9 ± 0.6	5.9 ± 4.6	8.0 ± 8.0	3.8 ± 1	9.6 ± 1.3	4.9 ± 0.2	15.38	70.7
NGC 6171 ¹	1.4 ± 0.6	2.7 ± 0.2	3.8 ± 1.1	6.4 ± 1.5	3.2 ± 1	30.8 ± 5.2	4.9 ± 0.2	23.01	-33.6
NGC 6218 ²	3.3 ± 0.9	1.4 ± 0.5	4.7 ± 1.2	4.9 ± 1.4	1.8 ± 1	34.5 ± 4.4	4.9 ± 0.2	-42.20	25.71
NGC 6341 ¹	3.8 ± 0.7	3.1 ± 0.2	6.8 ± 2.4	10.0 ± 2.0	3.2 ± 1	20.6 ± 3.4	5.3 ± 0.2	34.86	-120.3
NGC 6656 ²	3.8 ± 1.3	3.3 ± 0.8	7.4 ± 1.7	11.1 ± 2.9	2.7 ± 1	58.6 ± 7.0	5.4 ± 0.2	-8.15	-146.3
NGC 6752 ²	3.5 ± 0.8	2.0 ± 0.3	10.7 ± 1.4	5.5 ± 0.9	3.7 ± 1	63.9 ± 7.8	4.9 ± 0.2	-23.87	174.7
NGC 6809 ²	1.1 ± 0.8	1.6 ± 0.5	16.0 ± 5.8	5.5 ± 2.0	2.7 ± 1	28.6 ± 3.6	4.9 ± 0.2	-29.35	206.0
NGC 7078 ¹	5.1 ± 1.6	3.0 ± 0.3	8.7 ± 1.4	12.0 ± 1.7	3.2 ± 1	127.5 ± 21.0	5.5 ± 0.2	-27.31	-107.0
NGC 7099 ^{1,2}	2.1 ± 0.4	2.0 ± 0.2	6.8 ± 1.1	6.7 ± 2.4	2.1 ± 1	53.4 ± 8.3	4.8 ± 0.2	-46.80	-185.0

The first three entries give the parameters of the fits to the observed projected velocity dispersion profiles and their confidence intervals, to data from the Scarpa et al. group ¹ and the Lane et al. group ². The fourth column gives an empirical estimate of the point where the average stellar acceleration drops below a_0 . Columns 5-7 give the half-light radius calculated from the surface density light profiles, the Newtonian tidal radius from the Galactic mass model and orbital calculations derived from observed proper motions by Allen et al. (2006), and the total masses derived from the M/L values inferred through stellar population modelling by McLaughlin & van der Marel (2005) for each cluster, with corresponding confidence intervals. The last two columns give the galactic latitude of the clusters, and the radial velocity difference with respect to the Sun.

Given that the inclusion of even a few high-velocity contaminating stars can bias the velocity dispersion measurements significantly, e.g. Giersz & Heggie (2011), it is important to assess the robustness of the velocity dispersion profiles we use to this possibility. The stars from the Lane et al. group were selected through the requirement of four stellar parameters, ensuring membership through requiring simultaneously a ΔV_r , and also Ca , g and $[m/H]$ membership criteria. These makes it unlikely that contamination issues might have degraded the velocity dispersion profiles reported by the Lane et al. group. Regarding the Scarpa et al. results, only a ΔV_r membership criteria was used. However, as can be seen from the table, only one of their clusters, NGC 6171, has $|b| < 45$ and $\Delta V_r < 100 km/s$, showing that with this only possible exception, contamination of field stars is unlikely to affect the derived velocity dispersion determinations we use. It is also reassuring of the reliability of the Scarpa et al. results, that of the two clusters which have also been studied by the Lane et al. group, NGC

7099 has reported velocity dispersion profiles which are fully consistent when comparing the data samples from the two groups of observers. The case of NGC 288 has already been discussed, although both data samples are still consistent to within their respective errors, a definitive trend appears for large and small asymptotic velocity dispersion values for the Scarps et al. and Lane et al. groups, respectively

To summarise, we have tested the Newtonian explanation of Galactic tides as responsible for the observed $\sigma(R)$ phenomenology, and found it to be in tension with the observations, given the tidal radii (at perigalacticon) which the GCs in our sample present, are generally larger than the points where $\sigma(R)$ flattens, on average, by factors of 4, with values higher than 8 also appearing. An explanation under a MONDian gravity scheme appears probable, given the correlations we found for the clusters in our sample, all in the expected sense, and shown in Figures (1)-(7). Table (1) gives the parameters of velocity dispersion fits and their confidence intervals. The errors in σ_∞ are uncorrelated

with those in the other two parameters, which as it is easy to see from the model, are perfectly anti-correlated amongst themselves. The masses come from integrating the observed surface density light profiles, and using the M/L values, and their uncertainties, calculated using detailed stellar population modelling on a cluster by cluster basis by McLaughlin & van der Marel (2005).

5 CONCLUSIONS

From a purely empirical perspective, we test the Newtonian explanation of Galactic tides as responsible for the observed flattening of the velocity dispersion profiles in the GCs studied. These clusters can be shown to have Newtonian tidal radii at closest galactic passage larger than the points where $\sigma(R)$ flattens, by large factors of 4 on average, making the explanation under the Newtonian hypothesis suspect.

Through a careful modelling of the observed velocity dispersion profiles, we corroborate an average correlation between the appearance of a flat region in $\sigma(R)$ and the crossing of the a_0 threshold, as expected under modified gravity schemes.

By including results from careful stellar population modelling of the globular clusters studied to derive total mass estimates, we show that the asymptotic values of the measured velocity dispersion profiles, σ_∞ , and total masses for these systems, M , are consistent with the generic modified gravity prediction for a scaling $\sigma_\infty^4 \propto M$.

Although individual velocity dispersion profiles can be adequately fitted with either Newtonian Plummer models, or MONDian asymptotically flat ones to equivalent accuracy, the large Newtonian tidal radii sometimes found and the "Tully-Fisher" mass-velocity scaling observed, show that the phenomenology of the velocity dispersion profiles of the globular clusters studied is consistent with a qualitative change in gravity in the low acceleration regime, as predicted by MONDian gravity theories.

ACKNOWLEDGEMENTS

The authors thank an anonymous referee for a thorough reading of a previous version of the paper, leading to a helpful report abundant in constructive criticism. Xavier Hernandez acknowledges financial assistance from UNAM DGAPA grant IN103011. Alejandra Jiménez acknowledges financial support from a CONACYT scholarship.

REFERENCES

Allen C., Moreno E., Pichardo P., 2006, *ApJ*, 652, 1150
 Allen C., Moreno E., Pichardo P., 2008, *ApJ*, 674, 237
 Angus G. W., 2008, *MNRAS*, 387, 1481
 Bernal T., Capozziello S., Hidalgo J. C., Mendoza S., 2011, *Eur. Phys. J. C*, 71, 1794
 Bekenstein J. D., 2004, *Phys. Rev. D*, 70, 083509
 Binney, J., Tremaine, S., 1987, *Galactic Dynamics* (Princeton University Press, Princeton, NJ)
 Capozziello S., De Laurentis M., 2011, *Phys. Rep.* 509, 167
 Drukier et al., 1998, *AJ*, 115, 708
 Famaey B., McGaugh S., 2012, *Living Reviews in Relativity*, in press, arXiv:1112.3960

Giersz M., Heggie D. C., 2011, *MNRAS*, 410, 2698
 Haghi H., Baumgardt H., Kroupa P., Grebel E. K., Hilker M., Jordi K., 2009, *MNRAS*, 395, 1549
 Haghi H., Baumgardt H., Kroupa P., 2011, *A&A*, 527, A33
 Harris W. E., 1996, *AJ*, 112, 1487
 Hernandez X., Mendoza S., Suarez T., Bernal T., 2010, *A&A*, 514, A101
 Hernandez X., Jiménez M. A., Allen C., 2012, *EPJC*, 72, 1884
 Hernandez X., Jiménez M. A., 2012, *ApJ*, 750, 9
 Kroupa P. et al., 2010, *A&A*, 523, 32
 Kroupa, P., 2012, *PASA* in press, arXiv:1204.2546
 Küpper A. H. W., Kroupa P., Baumgardt H., Heggie D. C., 2010, *MNRAS*, 407, 224
 Küpper A. H. W., Lane R. R., Heggie D. C., 2012, 420, 2700
 Lane R. R., Kiss L. L., Lewis G. F., Ibata R. A., Siebert A., Bedding T. R., Szkely P., 2009, *MNRAS*, 400, 917
 Lane R. R. et al., 2010a, *MNRAS*, 406, 2732
 Lane R. R., Kiss L. L., Lewis G. F., Ibata R. A., Siebert A., Bedding T. R., Szkely P., 2010b, *MNRAS*, 401, 2521
 Lane R. R. et al., 2011, *A&A*, 530, A31
 Lane R. R., Küpper A. H. W., Heggie D. C., 2012, *MNRAS*, 423, 2845
 Lee J., Komatsu E., 2010, *ApJ*, 718, 60
 McLaughlin D. E., van der Marel, R. P., 2005, *ApJS*, 161, 304
 Mendoza S., Hernandez X., Hidalgo J. C., Bernal T., 2011, *MNRAS*, 411, 226
 Milgrom M., 1983, *ApJ*, 270, 365
 Milgrom M., 1994, *ApJ*, 429, 540
 Moffat J. W., Toth V. T., 2008, *ApJ*, 680, 1158
 Niederste-Ostholt M., Belokurov V., Evans N. W., 2012, *MNRAS*, 422, 207
 Scarpa R., Marconi G., Gilmozzi R., 2004, *Proceedings of "Baryons in Dark Matter Halos"*. Novigrad, Croatia, 5-9 Oct 2004. Editors: R. Dettmar, U. Klein, P. Salucci. Published by SISSA, *Proceedings of Science*, <http://pos.sissa.it>, p.55.1
 Scarpa R., Marconi G., Gimuzzi R., Carraro G., 2007a, *A&A*, 462, L9
 Scarpa R., Marconi G., Gimuzzi R., Carraro G., 2007b, *The Messenger*, 128, 41
 Scarpa R., & Falomo R., 2010, *A&A*, 523, 43
 Scarpa R., Marconi G., Carraro G., Falomo R., Villanova S., 2011, *A&A*, 525, A148
 Sollima A., Nipoti C., 2010, *MNRAS*, 401, 131
 Sollima A., Bellazzini M., Lee J. W., 2012, *ApJ*, 755, 156
 Thompson R., Nagamine K., 2012, *MNRAS*, 419, 3560
 Trager, S.C., King, I.R., Djorgovski, S., 1995, *AJ*, 109, 218
 Zhao H., Famaey B., 2010, *Phys. Rev. D*, 81, 087304